Electronic Supplementary Information (ESI†)

Colorimetric and "off-on" fluorescent Pd^{2+} chemosensor based on rhodamine-ampyrone conjugate: synthesis, experimental and theoretical studies along with *in vitro* applications

Sanchita Mondal,[*a] Saikat Kumar Manna,[*b] Sudipta Pathak,[*b] Abdulla Al Masum[c] and Subrata Mukhopadhyaya [a]

[a]Department of Chemistry, Jadavpur University, Kolkata 700032, India.

[b]Department of Chemistry, Haldia Government College, Debhog, Purba Medinipur, West Bengal 721657, India.

[c]Department of Life Science & Bio-technology, Jadavpur University, Kolkata 700032, India.

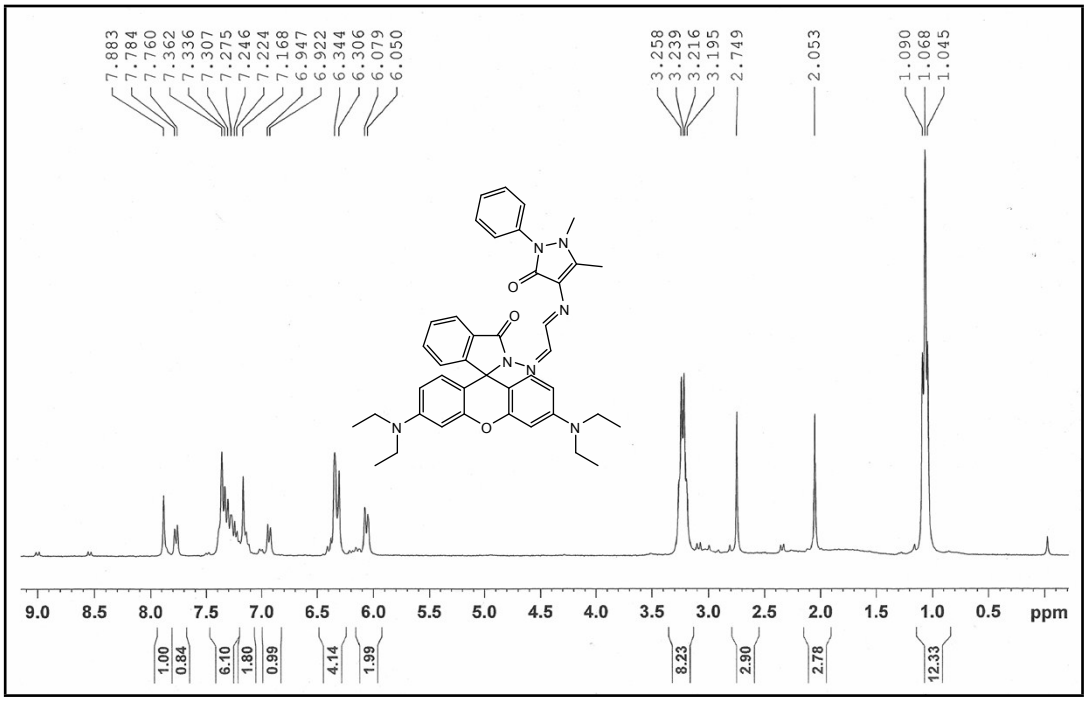

Figure S1: ^{1}H NMR spectrum of compound **L**.

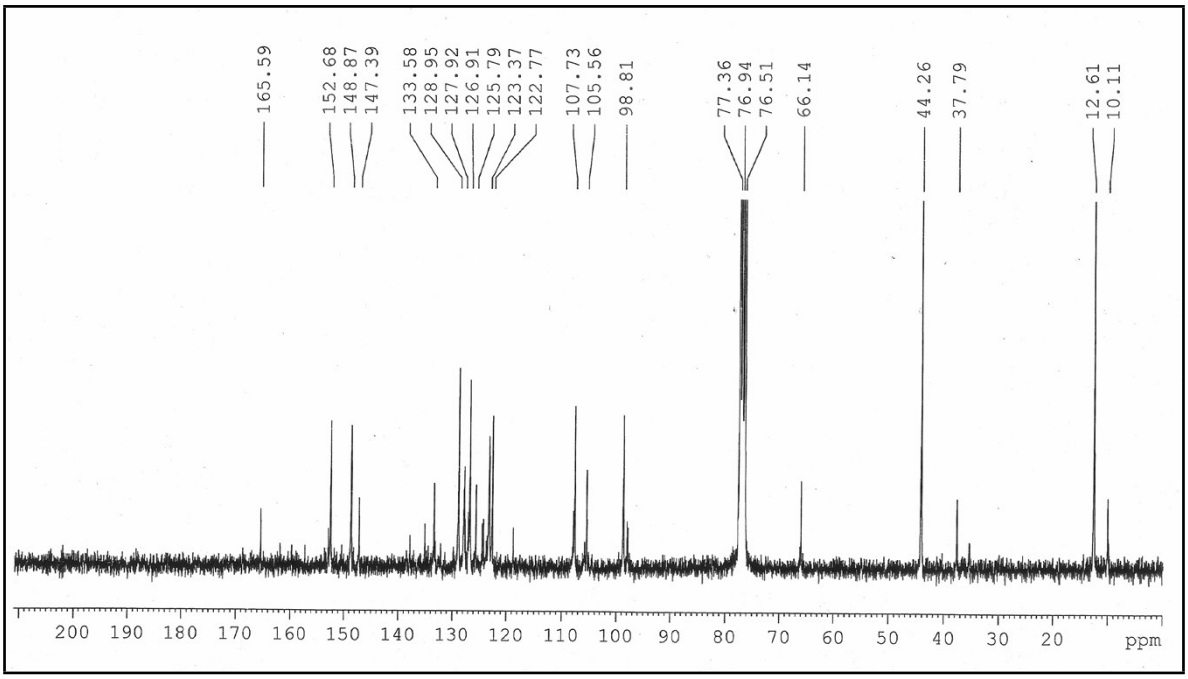

Figure S2: ^{13}C NMR spectrum of chemosensor **L**.

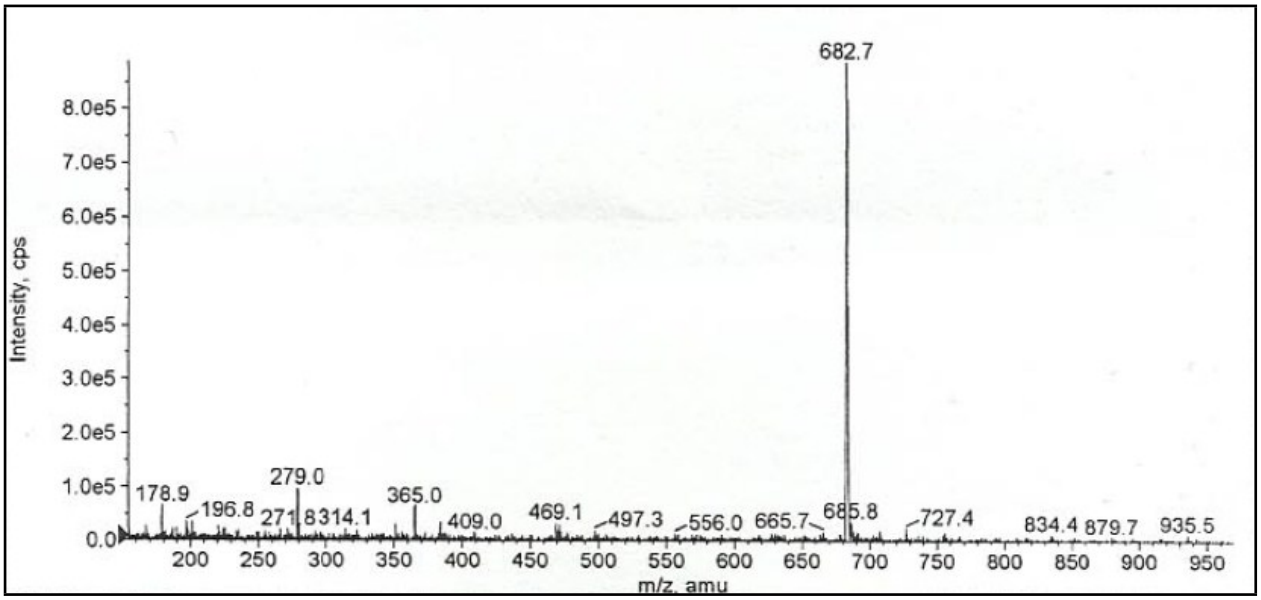

Figure S3: Mass spectrum of chemosensor **L**.

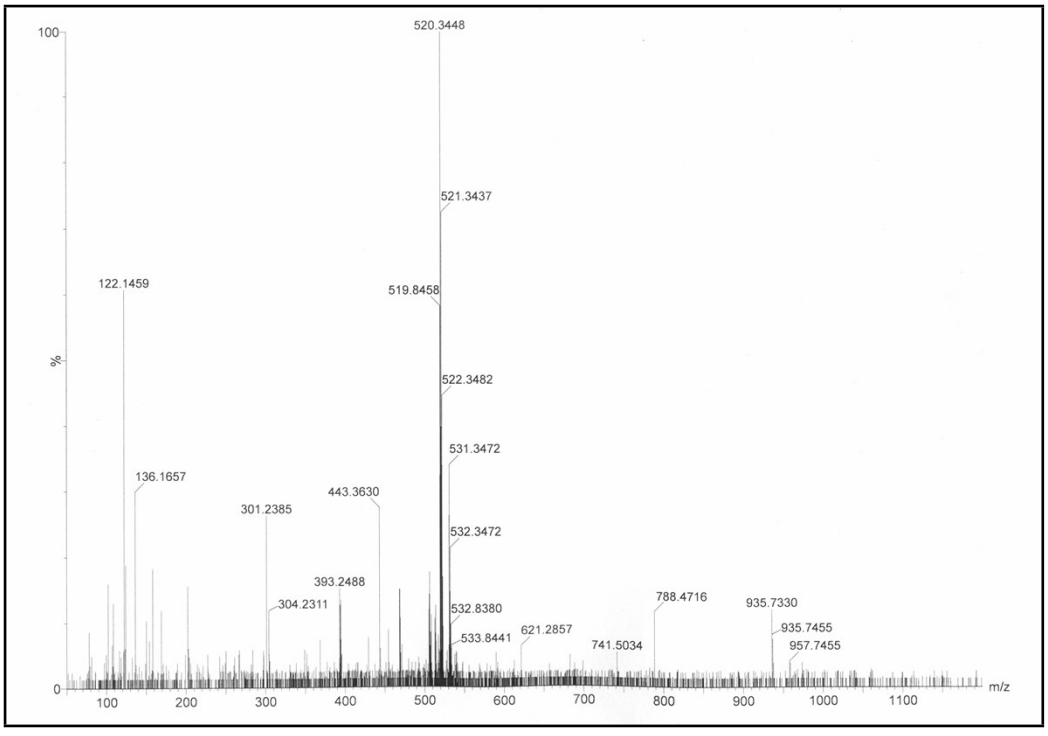

Figure S4: Mass spectrum of chemosensor **L**-Pd^{2+} complex.

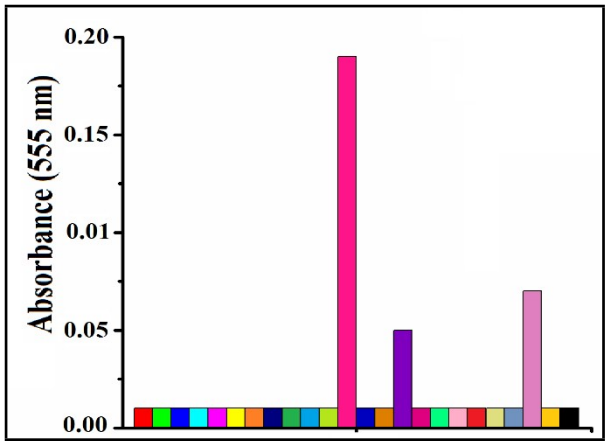

Figure S5: Change in the absorption spectrum of receptor **L** [c = 4× 10^{-5} M, CH_3CN/H_2O = 1 :1, v/v, 10 mM HEPES buffer, pH = 7.4) with respective metal cations (c = 4× 10^{-4} M, left to right- **L**, K^+, Na^+, Mg^{2+}, Ca^{2+}, Sr^{2+}, Ba^{2+}, Cr^{3+}, Mn^{2+}, Fe^{2+}, Fe^{3+}, Pd^{2+}, Co^{2+}, Ni^{2+}, Cu^{2+}, Zn^{2+}, Cd^{2+}, Pb^{2+}, Hg^{2+}, Pt^{2+}, Pd^0, Al^{3+}, Ru^{3+}, and Ag^+).

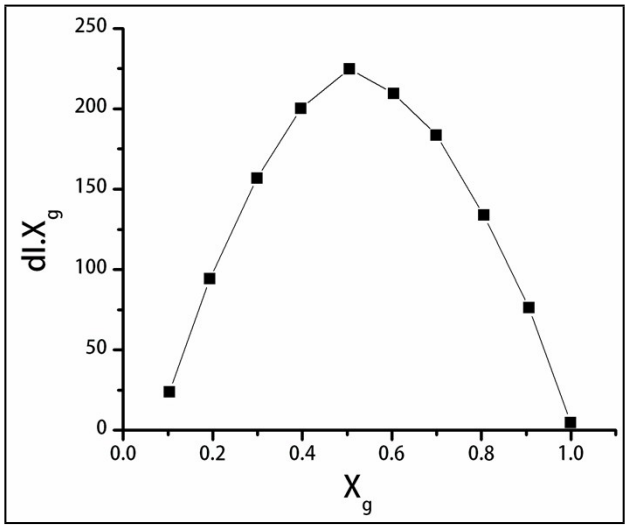

Figure S6: Fluorescence Job's plot for **L** with Pd^{2+} in CH_3CN/H_2O solution (8:2, v/v, 10 mM HEPES buffer, pH 7.4). ([H] = [G] = 4 × 10^{-5} M).

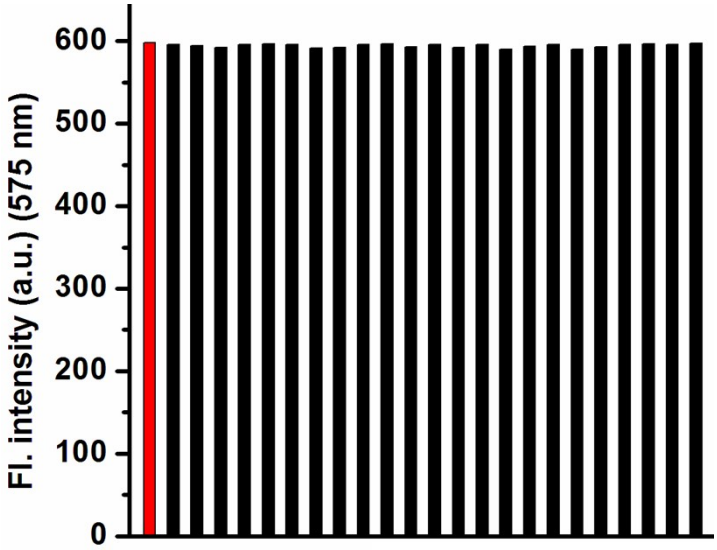

Figure S7: Fluorescence response of **L** (c = 1.0×10^{-5} M) to 1.0 equiv addition of Pd^{2+} (the red bar portion) and to the mixture of 10 equiv. of other metal ions with 1.0 equiv. of Pd^{2+} (the black bar portion, left to right- K^{+}, Na^{+}, Mg^{2+}, Ca^{2+}, Sr^{2+}, Ba^{2+}, Cr^{3+}, Mn^{2+}, Fe^{2+}, Fe^{3+}, Co^{2+}, Ni^{2+}, Cu^{2+}, Zn^{2+}, Cd^{2+}, Pb^{2+}, Hg^{2+}, Pt^{2+}, Pd^{0}, Al^{3+}, Ru^{3+}, and Ag^{+}).

Calculation for Limit of Detection (LOD):

The LOD of **L** for Pd^{2+} was determined using the following equation:

LOD = 3Sbl/S, Sb1 is the standard deviation of the blank solution; S is the slope of the calibration curve.

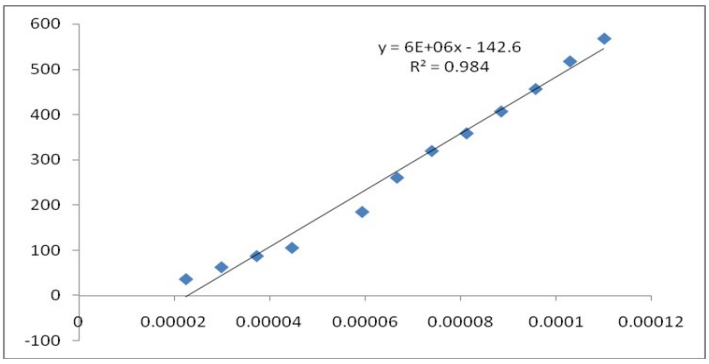

Figure S8: Calibration curve for fluorescence titration of **L** with Pd^{2+}.

From the graph we get slope (S) = 6×10^{6} Standard deviation (Sb1 = 23.81723)

Thus, using the formula, we get the LOD = 11.9×10^{-6} M = 11.9 µM.

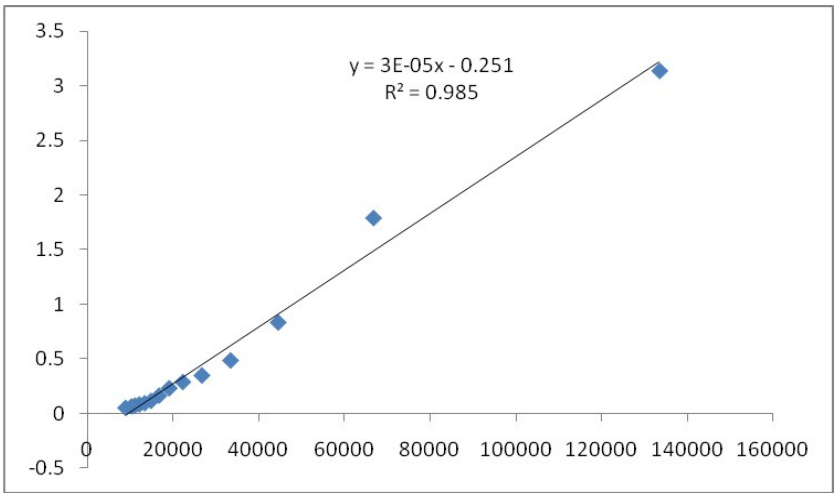

Figure S9: Bensei-Hildebrand plot obtained from the Fluorescence (emission calculated from 575 nm) studies. Binding constant ($K_a = 8.36 \times 10^3\ M^{-1}$) curve of sensor **L** with Pd^{2+} determined by fluorescence method.

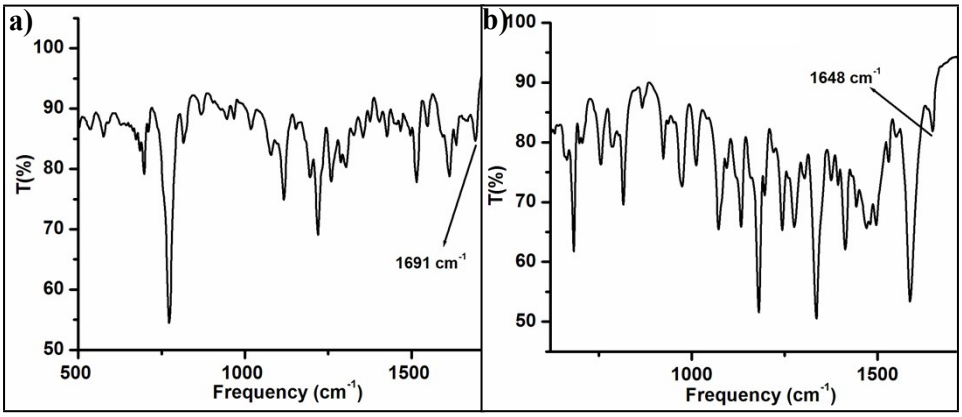

Figure S10: FTIR spectra of (a) **L** and (b) **L**-Pd^{2+} complex.

Theoretical study:

Table S1. HOMO-LUMO energy calculated for **L1** and **L1**-2Zn^{2+} complex using [(B3LYP/6-311G(d,p)] for **L** and B3LYP/LanL2DZ for **L**-Pd^{2+} for level of theory)

Species	E(HOMO)	E(LUMO)	ΔE(Hartree	ΔE(eV)	ΔE(kcal/mol)
L	-0.18937	-0.06438	0.12499	3.401	78.43
L-Pd^{2+}	-0.35355	-0.30237	0.05118	1.3927	32.11

1 Hartree = 27.2116 eV, 1 Hartree = 627.5095 kcal mol^{-1}

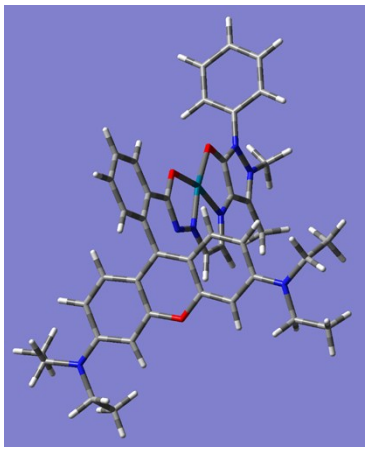

Figure S11: Energy-minimized structure of **L**-Pd^{2+} complex (atom color: gray = C, red = O, blue = N, white = H, teal blue = Pd).

Table S2: Selected bond length and bond angles in B3LYP/LanL2DZ optimized geometry of **L**-Pd^{2+}.

Bond	**Bond length (Å)**
Pd-O (rhodamine carbonyl)	2.09
Pd-N (rhodamine imino)	1.96
Pd-O (antipyrine carbonyl)	2.16
Pd-N (antipyrine inamine)	2.02

LUMO+2	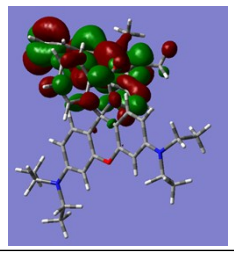	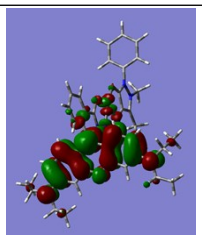
LUMO+1	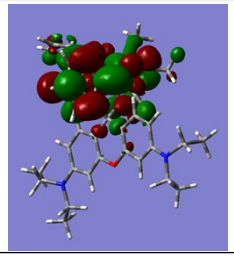	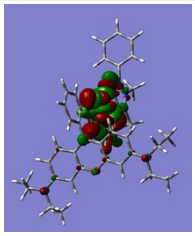
LUMO	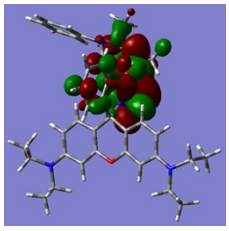	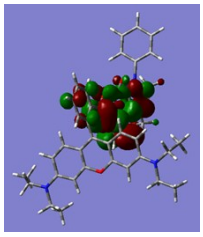
HOMO	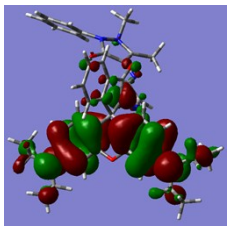	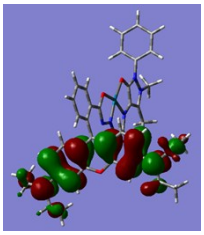
HOMO-1	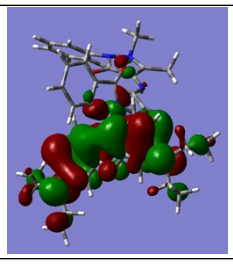	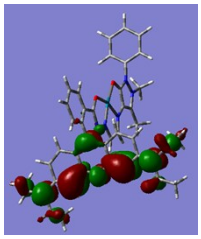
HOMO-2 **L**	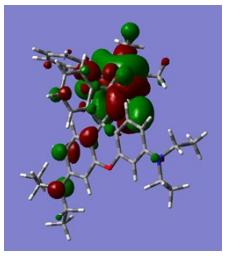	**L**-Pd^{2+} 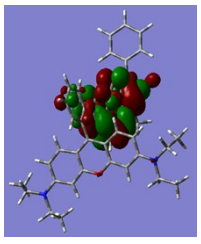

Figure S12: Molecular orbital plots of **L** and **L**–Pd^{2+}.

Cell imaging study:

Minimum Inhibitory Concentration (**MIC**): We have treated probe **L** with both gram positive and gram-negative bacteria. After 24 hrs. of treatment probe **L** shows no effect on gram negative bacteria but it showed some effect on gram positive bacteria. Probe **L** showed bactericidal activity on 100 µM.

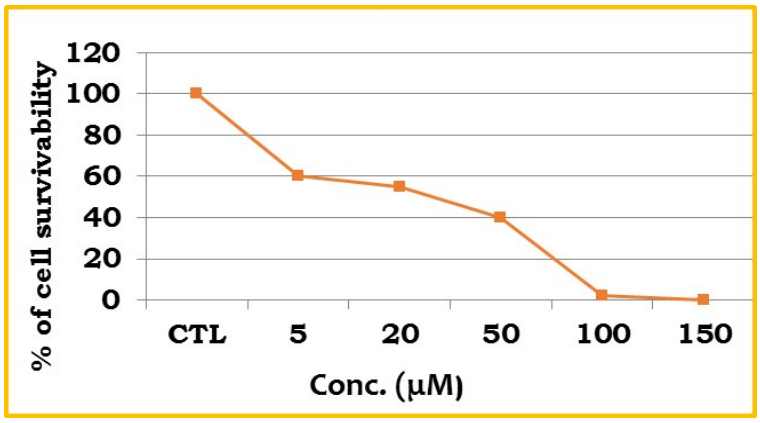

Figure S13: Minimum inhibitory concentration of compound against gram positive bacteria.

Cell Survivability Assay: Probe **L** showed cytotoxity against MDA-MB 468 cells when treated with different concentrations 0 - 150 µM for 24 hrs and cell survivability was determined by MTT assay. As seen in Figure S14 cell survivability decreased with increasing concentration of probe **L**. From the graph we also calculated LD_{50} and found that the value was 50 µM approx. for the probe **L.**

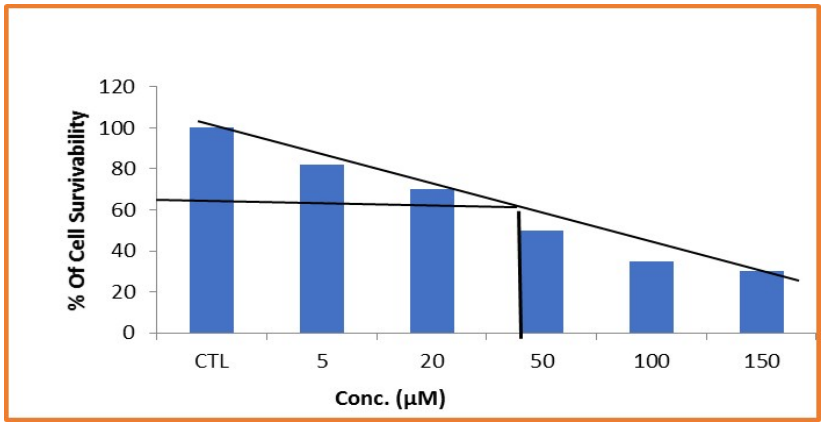

Figure S14: Cytotoxic effect of probe **L** on MDA-MB-468 cells. Cells were incubated with increasing concentrations probe **L** and its survivability was assessed by MTT assay.

Table S3. Summary of representative fluorescent probes for Pd^{2+}

Sl. No.	Chemical Structure	Media	Pd^{2+} limit of detection	Biological application
1.	**Our Work** 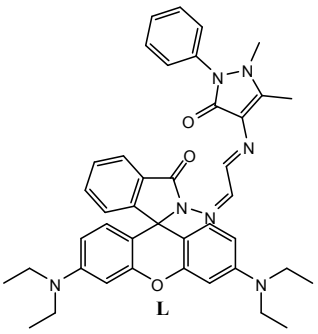 **L**	CH_3CN/H_2O (4:1, v/v, 10 mM HEPES buffer, pH 7.4)	11.9 μM	Our chemosensor can detect intracellular Pd^{2+} ion in MDA-MB-468 cells.
2.	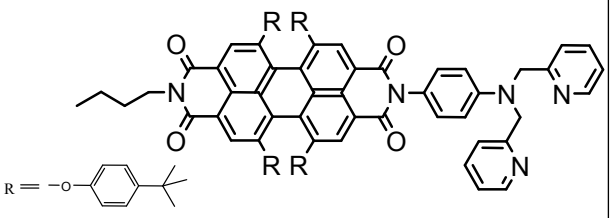 (*Tetrahedron,* 2014, **70**, 1997-2002)	DMF/H_2O (v/v, 7/1)	7.32 ppb (5.53 μM)*[1]	Not mentioned
3.	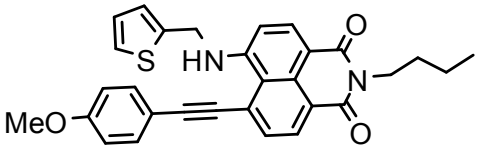 (*Chem. Commun*., 2008, 6339–6341)	Ethanol–water (60 : 40, v/v) solution at pH 7.2	Not mentioned	Not mentioned
4.	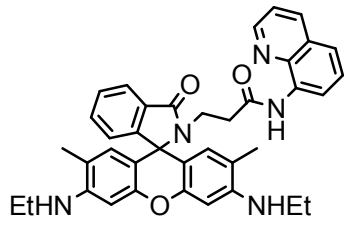 (*Chem. Commun*., 2011, **47**, 9101–9103)	EtOH–H_2O (1 : 1, v/v, 25 1C) at pH 7.2 (50 mM HEPES buffer)	Not mentioned	Not mentioned
5.	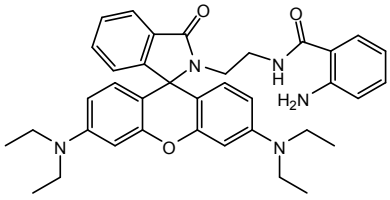 (*Dalton Trans.*, 2014, **43**, 4626–4630)	EtOH–H_2O (1 : 1, v/v)	73.8 nM (0.0738 μM) *[2]	Not mentioned

6.	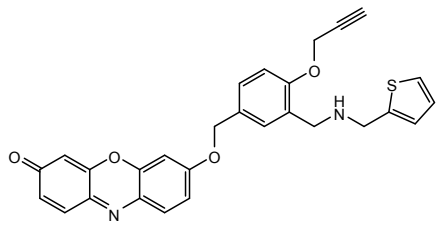 (*Sens. Actuators, B* 2012, **171– 172**, 1277– 1282)	MeOH/PBS (pH = 7.4, 10 mM) solution (8:2, v:v),	0.05 μM*[3]	Not mentioned
7.	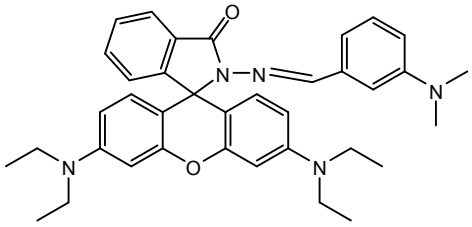 *(Sens. Actuators, B* 2012, **171– 172**, 508– 514)	HAc–NaAc buffer solution (pH = 4.7)	0.13 μM*[4]	Not mentioned
8.	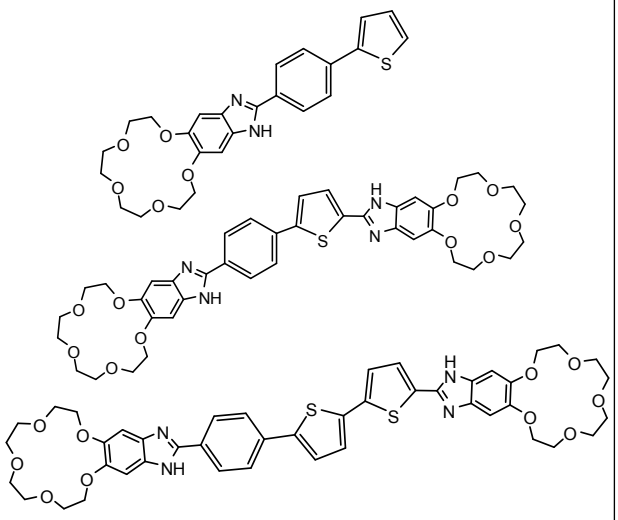 (*Tetrahedron* 2011, **67**, 7106-7113)	MeCN/DMSO (99:1)	Not mentioned	Not mentioned
9.	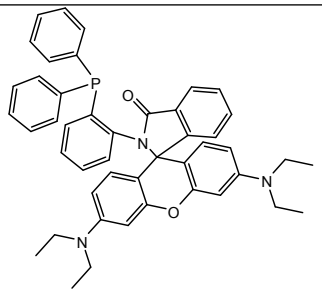 *(Chem. Commun.,* 2013, **49**, 822-824)	Ethanol–water (4 : 1, v/v),	1.49×10^{-9} M (1.49×10^{-3} μM)*[5]	Not mentioned

10.	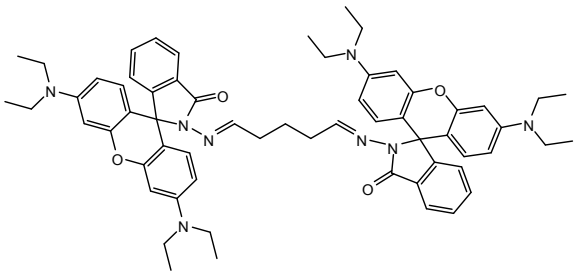 (*Analyst*, 2017, **142**, 1536–1544)	CH_3CN : H_2O (3 : 2 v/v)	1 μM*[6]	Not mentioned
11.	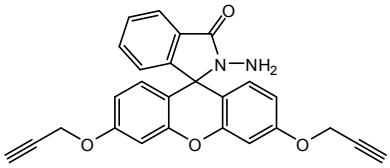 (*Tetrahedron Lett.* 2012, **53**, 3459–3462)	PBS (20 mM, pH 7.4) solution containing 10% (v:v) CH_3CN	Not mentioned	Not mentioned

*[1] Molecular weight of fluorophore is too high compared to **L** (**our work**). Thus, it is less important with respect to atom economy though its limit of detection is less than L

*[2] Overall yield of reported compound formation (37% in last step) is low compared to the synthesis of **L**.

*[3] The number of steps for the synthesis of fluorescent probe is more and some of the steps are low yielding (24%-75%).

*[4] Experiments were carried out at acidic condition (pH = 4.7). But biological pH is generally close to neutral. Thus, this method has much lower significance for Pd^{2+} contaminated cell.

*[5] Final step is low yielding (25%).

*[6] Yield of the final step is not high (55%). Due to large size of the molecule, it is less important in terms of atom economy too.

*[1-6] None of the tabulated methods above, except ours, were silent about their applications on living cells.